Author Manuscript
Author Manuscript
Author Manuscript
Author Manuscript

HHS Public Access
Author manuscript
Fuel (Lond). Author manuscript; available in PMC 2018 March 19.

Published in final edited form as:
Fuel (Lond). 2015 May 15; 148: 87–97. doi:10.1016/j.fuel.2015.01.046.

Stochastic reservoir simulation for the modeling of uncertainty in coal seam degasification

C. Özgen Karacan[a,*] and **Ricardo A. Olea**[b]

[a]NIOSH, Office of Mine Safety and Health Research, Pittsburgh, PA, United States

[b]USGS, Eastern Energy Resources, Reston, VA, United States

Abstract

Coal seam degasification improves coal mine safety by reducing the gas content of coal seams and also by generating added value as an energy source. Coal seam reservoir simulation is one of the most effective ways to help with these two main objectives. As in all modeling and simulation studies, how the reservoir is defined and whether observed productions can be predicted are important considerations.

Using geostatistical realizations as spatial maps of different coal reservoir properties is a more realistic approach than assuming uniform properties across the field. In fact, this approach can help with simultaneous history matching of multiple wellbores to enhance the confidence in spatial models of different coal properties that are pertinent to degasification. The problem that still remains is the uncertainty in geostatistical simulations originating from the partial sampling of the seam that does not properly reflect the stochastic nature of coal property realizations. Stochastic simulations and using individual realizations, rather than E-type, make evaluation of uncertainty possible.

This work is an advancement over Karacan et al. (2014) in the sense of assessing uncertainty that stems from geostatistical maps. In this work, we batched 100 individual realizations of 10 coal properties that were randomly generated to create 100 bundles and used them in 100 separate coal seam reservoir simulations for simultaneous history matching. We then evaluated the history matching errors for each bundle and defined the single set of realizations that would minimize the error for all wells. We further compared the errors with those of E-type and the average realization of the best matches. Unlike in Karacan et al. (2014), which used E-type maps and average of quantile maps, using these 100 bundles created 100 different history match results from separate simulations, and distributions of results for in-place gas quantity, for example, from which uncertainty in coal property realizations could be evaluated.

The study helped to determine the realization bundle that consisted of the spatial maps of coal properties, which resulted in minimum error. In addition, it was shown that both E-type and the

*Corresponding author. Tel.: +1 412 3864008. cok6@cdc.gov (C. Özgen Karacan).

Disclaimer

This paper has been peer reviewed and approved for publication consistent with U.S. Geological Survey Fundamental Science Practices (http://pubs.usgs.gov/circ/1367/). For the National Institute for Occupational Safety and Health (NIOSH), the findings and conclusions in any paper are those of the authors and do not necessarily represent the views of NIOSH. Mention of any company name, product, or software does not constitute endorsement by NIOSH or USGS.

Author Manuscript Author Manuscript Author Manuscript Author Manuscript

average of realizations that gave the best match for invidual approximated the same properties resonably. Moreover, the determined realization bundle showed that the study field initially had 151.5 million m^3 (cubic meter) of gas and 1.04 million m^3 water in the coal, corresponding to Q90 of the entire range of probability for gas and close to Q75 for water. In 2013, in-place fluid amounts decreased to 138.9 million m^3 and 0.997 million m^3 for gas and water, respectively.

Keywords

Coal seam gas; History matching; Geostatistics; Sequential simulation; Realization; Mean square error

1. Introduction

Coal seam degasification is an important practice for minable coal seams for two reasons; the first is its proven effectiveness in improving the safety of underground coal mines by reducing the risk of methane explosions through a reduction in coal gas content, and the second is the potential of utilizing produced methane as an unconventional energy source either as pipeline gas or to generate electricity at the mine site [15,23].

It is widely recognized that ventilation of underground coal mines with an adequate amount of dilution air is important to prevent formation of explosive methane–air mixtures. However, when gas contents of coal seams are high, or their structural and reservoir properties favor high methane emissions, ventilation alone may not be enough to keep methane levels within statutory limits, thus increasing the potential for methane ignitions. Coal gas extraction developed in the 70s in the Oak Grove field of the Black Warrior Basin in Jefferson County, Alabama, and initially was intended to reduce high gas content of the Mary Lee coal seam and thus reduce methane emissions into active mine workings. The results of these past efforts showed that methane production using vertical boreholes and combined with hydraulic fracturing significantly decreased frictional ignitions and methane explosion dangers in coal mining [8].

Coal seam gas drainage that started with mining safety in mind has drastically improved since the 70s: for optimum reservoir management, for effective gas injection and production in minable and unminable coal seams, gas capture from abandoned mines, and for gas production and geo-sequestration (e.g. [21,27,18,19,16,20,10,3,26]. Due to the socio-economic importance of these objectives, production analyses (e.g. [1] and coal bed reservoir simulation techniques have been developed and improved over the years, and have remained as one of the most dependable and effective methods of reservoir analysis and management [11]. This is especially true for coal seam reservoir models that are benchmarked using simultaneous multi-well history matching of well production.

The purpose of history matching, especially multi-well, is to gain confidence in the values of assigned coal properties and their distribution within the modeling domain of interest. However, coal seams are more heterogeneous compared to conventional oil or gas reservoirs, and properties that control fluid storage and flow may show significant variations even over small distances [17]. Establishing multiple coal properties and assigning uniform values to

Author Manuscript Author Manuscript Author Manuscript Author Manuscript

match observed productions are deterministic, time consuming, and ultimately may not be effective for multi-well history matching. In order to address this problem and to be able to simultaneously history match multiple wells, Karacan et al. [12] modeled a coal seam degasification area in Indiana using geostatistics to produce average interpolated values for parameters and predictions from E-type realizations of coal properties. The approach included six years of production data from nine wells, allowing for effective simultaneous multi-well history matching. However, in Karacan et al. [12], full advantage of stochastic simulations was not taken advantage of by using E-type maps instead of individual realizations. E-type maps are the median-value map that is constructed by using all available realizations of the same property. They, therefore, can be considered as kind of average and do help assessing uncertainty in results with respect to other potential inputs.

Depending on the objective of the work, different applications of geostatistics can be merely an intermediate step rather than a final one. This is especially true if the purpose of generating geostatistical representations is to use them for flow studies. The objective of the present study is to expand previous geostatistical simulation results from Karacan et al. [12] by taking full advantage of geostatistics and stochastic simulations to address uncertainty that stems from partial sampling of the coal and from property realizations. For this purpose, 100 randomly generated realizations for each of the 10 properties were batched to create 100 bundles and were used in 100 separate reservoir simulations. Errors of each bundle in matching wellbore gas and water productions were evaluated to define the single set of realizations that would minimize error for all wells. The specific aim is to quantify uncertainty through minimization of history matching errors for single and multiple wells, thereby determining the most probable set of realizations for coal properties in the modeled area that could be used in all important calculations related to in-place fluid volumes and for making decisions related to degasification.

2. Description of the study and background information

This work is built upon some of the concepts and analyses performed in Karacan et al. [12]. Therefore, the detailed information related to the site, geology, coal and gas properties, and the producing wellbores will not be repeated in this paper. However, for completeness of this work, brief background information related to the study site, producing wellbores, data sources, and some of the analyses that have already been conducted and led to the present work are given in this section.

The producing wells and the area studied in this paper are located in the Indiana portion of the Illinois Basin, USA. The wells are located in Sullivan County (Fig. 1) and have been producing methane of mostly biogenic origin from the Seelyville coal seam since July of 2007. The Seelyville coal seam is within the Pennsylvanian aged formations of the Carbondale Group and occurs generally at depths between 150 and 200 m in Sullivan County, and contains high-volatile bituminous C and B rank coal (Fig. 1). Besides the Seelyville coal seam of the Linton Formation, other important seams in this stratigraphy are the Danville and Hymera coal seams of the Dugger Formation and the Springfield coal seam of the Petersburg Formation due to their thicknesses and lateral extents [22,7].

Author Manuscript Author Manuscript Author Manuscript Author Manuscript

Measurements of reservoir pressures and gas contents suggest that the Seelyville coal is saturated (in terms of gas adsorption equilibrium) with gas contents ranging from 1.25 to 4.25 m^3/ton. This gas is mostly methane (>95%), rich in biogenic origin. However, significant variations in the gas content can be expected in both the lateral and vertical directions [28]. The nine coalbed methane (CBM) wells studied in this work (Fig. 1) are not fractured due to high coal permeability. However, they had skin values determined from production analysis indicating a zone of negative (6 wells) and positive (3 wells) skin around the completions. These nine wells collectively produced approximately 15 million m^3 of this gas between July of 2007 and October of 2013, which was sold to a nearby pipeline. This period is the duration of the production data analyzed in this paper. Measured bottom-hole pressures and gas and water production rates, referred to as historical data, from 5 of these wells are shown in Fig. 2.

2.1. Brief description of the background work to link it to the current work and uncertainty assessment

Geostatistical approaches that generate realizations of important coal properties related to fluid storage and transport within the coal seams and the resultant reservoir simulations for history matching were driven by the actual data. Therefore, the work started with the examination of data availability and validation to identify modeling domains. The majority of the spatial coal properties such as thickness, depth, and ash-moisture were extracted from databases [5,6]. Other important data related to coal reservoir properties were determined by analyzing each well's gas and water production rates using Fekete's F.A.S.T. CBM™ software version 4.7 [9], and assuming a pseudo-steady state approach based on the long production periods. These properties included coal permeability, porosity, water saturation, relative permeability functions, and coal matrix shrinkage functions at individual well locations. Details of the data, data sources, and production data analyses of CBM wells are discussed in Karacan et al. [12].

To simulate coal seam reservoir production and to generate geostatistical realizations of coal properties, a model area was developed covering a 27.2-km^2 area with 7.25-km and 3.75-km lengths in x and y directions, respectively. The model area was divided into 75 and 145 nodes in x and y directions with a 50-m node spacing (Fig. 1).

Spatial data were conditionally simulated by using a sequential Gaussian simulation (SGSIM) and sequential Gaussian co-simulation (co-SGSIM) techniques to generate realizations of each of the coal properties using the Stanford University geostatistical modelling software package (SGeMS) [25]. One hundred realizations for each of the coal properties—permeability (x, y, z), cleat porosity, water saturation, thickness, depth, Langmuir volume (V_L) scaled for ash and moisture content, and pressure—were generated stochastically by changing the seed number between each of the realization-generation steps. In scaling Langmuir volume to as-received basis, methane isotherm reported on dry-ash-free basis (daf), was adjusted for the cumulative amount of moisture and ash content at data locations so that the V_L would represent as-received conditions and would include the volume-reducing effect of ash and moisture in maps used for production history matching. In addition, gas and water relative permeability as well as matrix shrinkage functions

Author Manuscript Author Manuscript Author Manuscript Author Manuscript

determined from the production analyses of each CBM well were assigned to the nodes of the generated Voronoi regions that represented the nearest neighborhood of a specific CBM well for those properties [12].

Generation of all geostatistical realizations by using the same number and size of the nodes and at the same node addresses as the reservoir simulation model grid made importing coal property maps into the reservoir simulation grid readily possible. Reservoir simulations for simultaneous history matching were performed using GEM v. 2007 [2] with a dual-porosity formulation and by operating the wells with measured bottom-hole pressure constraints.

The reservoir simulations performed and presented in Karacan et al. [12] used E-type maps of all coal property realizations and the average realization of the quantile realizations (Q-average) determined in every 10 quantiles between 5 and 95. The Q-average realizations were used as step-wise approximations to the E-type and to generate more realistic representations of the spatial distribution of coal properties to be used in reservoir simulations.

Although both E-type and Q-average maps of coal properties were successful for simultaneous history matching of gas and water productions of all wells, they did not effectively address the uncertainty associated with stochastic maps (100 in this case for each property). E-type and its proxy map, Q-average, cover uncertainty that can otherwise be assessed by using each individual realization in reservoir simulation for testing history matching errors. In fact, this is an advantage that the stochastic geostatistical simulations offer when the generated property maps are used in reservoir simulations [24]. This distinction is where this paper diverts in scope and content from our previous work [12] and thus connects to the objective of the current paper.

In this work, all 100 realizations of 10 different properties, not just the E-type, were used in 100 separate simulations in order to be able to assess errors and uncertainty, and to establish confidence intervals through distributions of parameters. In this regard, this work takes the full advantage of stochastic geostatistical simulations in coal seam reservoir studies and can be considered as an improvement over Karacan et al. [12].

3. Coal bed reservoir simulations of gas drainage using individual realization bundles and assessment of history matching errors

Generation of stochastic maps using different seed numbers prior to each simulation in SGSIM or co-SGSIM was random by the nature of the process [25,4]. Therefore, 100 stochastic realizations for each of the simulated and co-simulated coal variables made up 100 random bundles of property maps that could be used in 100 different reservoir simulations for assessing uncertainty through history matching errors. It should be reiterated that since the realizations were generated randomly by changing the seed number at the start of stochastic simulations of each coal properties, it was assumed that 100 realizations of each of the 10 properties were randomly sequenced to form 10 decks of 100 realizations. As the continuation of the random nature of stochastic processes and random sampling, initially we took the first realization from each set to build the first bundle, and then second from

Author Manuscript Author Manuscript Author Manuscript Author Manuscript

each set, and then the third and so forth, to create 100 bundles of random samples. We did not make a separate pre-sorting of realizations in attempt to form the best bundle. The best possibility was judged based on history match results.

In this work, the name of the bundle and its simulation results is denoted by the name of the realizations (real 15, for example). One hundred different realization bundles were created by assembling the corresponding realization numbers from each property set— e.g. real 15's from porosity, thickness, Langmuir volume, permeability, water saturation pressure, and depth—into a database so each bundle could be imported into the reservoir simulator for a new run.

Using each of the realization bundles and operating the wells with bottom-hole pressure values (Fig. 2), 100 reservoir simulations were performed to generate gas and water rates for each of the 9 wells. Fig. 3 shows, as an example, simulated gas and water rates for all 100 simulation runs (light-colored lines) as well as measured rates for wellbore Hall-1 (yellow circles).

The results shown in Fig. 3 reveal that the predicted rates differ based on the realization bundle used. This means that there is an error distribution associated with the uncertainty in realizations of coal properties. As a corollary to the distribution of the errors, it is reasonable to expect that there is only one realization bundle for each well that will result in the minimum average error when simulated rates are compared with the measured values, and that there is also one that will result in the maximum error. In between, there should be a mean and a standard deviation of errors calculated based on 100 results. In this work, the average error of simulated values compared to the measured ones was calculated using average root mean square of errors $(\overline{\mathrm{RMSE}})$ and by using the following relation:

$$\overline{\mathrm{RMSE}}=\sqrt{\frac{\sum_{j=1}^{n}(Q_j-Q_{\mathrm{hj}})^2}{n}} \quad (1)$$

In this equation, Q_j is the simulated rate at a particular date (j) and Q_{hj} is the measured (or historical) rate at the same date. The average is calculated by the number of date events (n = 75, in this case).

Calculating the average error between simulated and measured rates of gas and water for each wellbore for each simulation helps to delineate the error ranges with relevant basic statistics, such as minimum, maximum, mean, and standard deviation of errors. Calculating average errors for each simulation also helps to determine realization bundles that give minimum and maximum errors, and thus the best and worst scenarios of coal property distributions, in reservoir simulations for history matching. Although each realization is equi-probable in terms of representing the reality of property distributions, it is clear that only one of them is the correct, or close-to-correct, representation of reality in relation to the complex nature of fluid storage in coal seams and the flow dynamics during gas drainage. To follow the same wellbore given in Fig. 3 as an example, realization bundles 64 and 38 generated the minimum and maximum average errors, respectively, in gas rate prediction for

Author Manuscript Author Manuscript Author Manuscript Author Manuscript

Hall-1. Similarly, realization bundles 72 and 81 resulted in the minimum and maximum errors in water rate prediction for the same borehole. Simulated gas and water rates using these realization bundles as well as measured data are comparatively shown in Fig. 4 for Hall-1. Fig. 4 for Hall-1 and the data given in Table 1 for all wells show that there is a range of uncertainty in reservoir simulation results that stems from the uncertainties in realizations and their representativeness of the actual reservoir properties.

Additional information that can be observed in the data given in Table 1 is that the realization generating the best result for each wellbore is different. This means that each realization bundle that results in minimum matching error for each well is addressing the uncertainty at a local level, and only for the coal reservoir parameters within the volume that is affected by the pressure transients created by that wellbore. Therefore, as a corollary, it is clear that the best realization that is good for one wellbore will not create the same result for another since it will not address the coal properties at that location. This is an expected outcome for reservoir simulation conducted in a heterogeneous media like coal, and is a consequence of spatial distribution of fluid storage and flow-related properties. In fact, this very reason is also, if available data permits, why representative distributions of various properties should be used in reservoir simulations and why simultaneous multi-well history matching of gas and water rates should always be preferred over matches from a single wellbore to gain better insights about the coal seam.

In order to address the problem described above and the uncertainty associated with it, the first approach followed in this paper was to identify the single best realization bundle that would minimize the average error of simultaneous history matching for all wellbores. The second approach was to pick all 9 best realization bundles of each individual well that resulted in minimum error and average maps of corresponding coal properties to generate a single realization for the simulation. In the second approach, only the best realization bundles given for gas rates (Table 1) were used for the generation of an average. First, the measured gas rates were more continuous compared to the intermittent nature of water rates and second, the water rates were used as independent control data.

In order to identify the best realization bundle that would minimize the average history matching errors for all wells, Eq. (2) below was used. In this equation, the terms are similar to those of Eq. (1), except for the additional term "*m*," the number of wells, which averages the cumulative error accumulated from all wells. The well-number-averaged distribution of errors calculated using Eq. (2) is shown in Fig. 5.

$$\overline{\overline{\mathrm{RMSE}}}=\frac{\sum_{i=1}^{m}\left(\sqrt{\frac{\sum_{j=1}^{n}(Q_j-Q_{\mathrm{hi}})^2}{n}}\right)}{m} \qquad (2)$$

Fig. 5 shows that the average cumulative error based on the predictions of all wells ranged from 322.7 m^3/day (minimum) to 567.9 m^3/day (maximum) with a mean of 448.5 m^3/day and a standard deviation of 52.8 m^3/day. The minimum average error that would satisfy the entire modeling area and simultaneous history matching of all wells was determined by the

Author Manuscript Author Manuscript Author Manuscript Author Manuscript

simulation that utilized realization bundle 69, which can be considered as the most probable representation of the properties of the Seelyville coal seam in the study area amongst all 100 realization bundles.

The gas and water production rate errors predicted for individual wells by using realization 69 and the average of best realizations, as described above, are compared to those of E-type in Table 2. The data shown in this table indicates that the individual errors of the wells achieved by bundle 69, by average of the best realizations documented in Table 1 and by the E-type bundle, are not very different from what were documented in Table 1. It is also noticeable in Table 2 that the errors of the matching results between these three realizations are not too large either. Therefore, it may be a fair assessment to say that these three sets of realization bundles can actually satisfactorily represent the properties of the entirety of this area for simultaneous multi-well history matching of gas and water rates, with errors distributed in a narrow margin. The supporting evidence for this assessment is shown graphically in Fig. 6, where simulated water and gas rates are compared with the measured values for four of the wellbores: Arnett-2, Arnett-3, Hall-1, and McCammon.

Slightly better error distribution in Table 2 with E-type, compared to realization 69, can be due to the smoothing effects of these two in coal properties, especially around the wellbores. Better errors with the average of best realizations can be a combination of eliminating most of the realization bundles, except for the 9 best, which may not be a true representation of the field and which may also due to smoothing.

The ultimate purpose of history matching is to estimate important reservoir parameters, and to make subsequent production and reservoir management decisions. In addition, once these properties and their distributions within the field are determined, they can be used to perform calculations related to total gas-in-place (GIP) as well as in-place water quantity. These volumes are important for project development and for mine safety when the purpose of degasification is to reduce gas content prior to coal mining.

In this work, fluid-in-place volumes were computed for all 100 realization bundles by following the approach presented in Karacan et al. [13], Karacan [16], and in Karacan and Olea [14] for gas, and using the water-occupied portion of the pore volume for water. These values for each realization bundle were then used to determine basic statistics and the quantiles of the distributions to establish the confidence interval and to assess uncertainty. The histograms of these quantities, as well as their basic statistics and the quantiles of these distributions, are shown in Fig. 7 and given in Table 3, respectively.

The basic statistics of these distributions and the values at different quantiles, which are given in Table 3, show that initial GIP in this area ranged between 112.4 million m^3 and 172.4 million m^3, whereas water quantity in coal cleats ranged between 0.73 and 1.16 million m^3. As the result of degasification between 2007 and 2013 using these 9 wellbores, GIP shifted to lower values between 105 and 160 million m^3 and water amount decreased to potential values between 0.71 and 1.13 million m^3. More importantly, since the uncertainty assessment of coal properties based on history matching errors showed that realization 69, E-type, and average of best realizations are the most likely representations of the coal

Author Manuscript Author Manuscript Author Manuscript Author Manuscript

properties, GIP and water in coal cleats within the study area were computed for those realizations too (Table 4). Gas and water quantities calculated based on these realizations—specifically realization 69 and how the values of spatial properties evolved over time due to gas drainage—show that the field initially had 151.5 million m^3 of gas and 1.04 million m^3 of water in the coal. These values correspond to Q90 of the entire range of probabilities for gas and close to Q75 for water. In 2013, in-place fluid amounts calculated using realization 69 decreased to 138.9 million m^3 and 0.997 million m^3 for gas and water, respectively. These quantities are close to Q50 of the initial distribution (close to Q90 of the final distribution) for gas, and Q75 of the initial and final distributions for water.

Finally, Fig. 8 shows some of the coal properties from realization 69, E-type, and average of the best realizations for comparison purposes. The first row of images is the coal cleat volumes within the study area, calculated by multiplying area by thickness and porosity realizations. The second row is the permeability and the third is the Langmuir volume for methane. It is clear in these realizations that, ignoring the smoothing effects due to averaging between realizations, these maps carry similar characteristics in terms of spatial distribution of values and so they generate similar gas and water rate predictions and similar prediction errors. Similar templates of maps for these three realizations are given for coal pressure in Fig. 9. In this figure, distributions of the initial properties in 2007 are presented, in addition to distributions as of 2013 resulting from degasification. These figures show, again, that although the pressure change patterns are generally similar, they show slight spatial variability based on the variability of other reservoir properties, such as permeability and water saturation, within realization 69, E-type, and the average.

The uncertainity analyses presented in this discussion based on history matching errors showed that the realization 69 bundle consisted of the spatial maps of coal properties that resulted in simultaneous history matching of all wellbores for gas and water by generating the minimum amount of matching errors. Based on this result, distribution of coal properties within the model could be determined and uncertainty in GIP and in-place water could be assessed for better field management. Results also showed that both E-type and the average of realizations that gave the best match for invidual wells approximated the same properties resonably well.

4. Summary and conclusions

Geostatistical realizations of coal properties were generated using sequential Gaussian simulation and co-simulation techniques using spatial data from databases [12]. In this work, instead of using only the E-type map in simulations, 100 realizations randomly generated for each of the 10 properties were batched to create 100 bundles. These bundles of realizations were imported into reservoir simulations for 100 separate runs, and history matching errors of gas and water productions for each bundle were evaluated to define the single set of realizations that would minimize the error for all wells. Therefore, this work takes full advantage of stochastic simulations and extend previous findings to distributions, from which uncertainity can be assessed and confidence intervals can be defined. In this regard, this work improves previous findings of Karacan et al. [12] in the realm of uncertainty.

Author Manuscript Author Manuscript Author Manuscript Author Manuscript

Uncertainity analyses based on errors showed that the realization 69 bundle consisted of the spatial maps of coal properties that resulted in minimum error. In addition, it was shown that both E-type and the average of realizations that gave the best match for invidual wells approximated the same properties resonably well. Based on these results, it was concluded that the presented approach was effective in selecting maps of coal depth, coal thickness, porosity, water saturation, horizontal and vertical permeabilities, Langmuir volume, coal matrix, and cleat pressures. These properties are important for fluid flow and gas storage in coal seams to evaluate the initial conditions as well as to assess how gas and water quantity change or redistribute within the field as the result of degasification. The realizations of some of these properties were presented in the paper in comparison to E-type and to the average of best realizations.

In addition, the maps that represent the most likely conditions of a coal seam can be used to compute spatial or overall gas content, water- and gas-in-place before and after degasification to evaluate uncertainty within the numerical probability distribution with confidence intervals. For instance, the study field initially had 151.5 million m^3 of gas and 1.04 million m^3 water in the coal, corresponding to Q90 of the entire range of probability for gas and close to Q75 for water. In 2013, in-place fluid amounts decreased to 138.9 million m^3 and 0.997 million m^3 for gas and water, respectively. These quantities are close to Q50 of the initial distribution (close to Q90 of final distribution) for gas, and to Q75 of initial and final distributions for water. Such an evaluation is not only important for project economics and to decide whether additional wells should be drilled, but also for improving mining safety through integrating potential methane emissions into the ventilation plan at the time of considering the coal for mining.

Acknowledgments

We are very grateful to Larry Neely and Maverick Energy for access to production data for CBM wells. Drs. Maria Mastalerz and Agnieszka Drobniak are also thanked for their help in data gathering.

References

1. Clarkson CR. Production data analysis of unconventional gas wells: review of theory and best practices. Int J Coal Geol. 2013; 109–110:101–46.
2. Computer Modeling Group Ltd. Generalized equation of state model-GEM user's guide. Calgary (Alberta, Canada): 2007.
3. Connell LD, Detournay C. Coupled flow and geomechanical processes during enhanced coal seam methane recovery through CO_2 sequestration. Int J Coal Geol. 2009; 77(1–2):222–33.
4. Deutsch, CV., Journel, AG. GSLIB geostatistical software library and user's guide. 2. Oxford University Press; 1998. p. 369
5. Drobniak A, Mastalerz M. The Indiana geological survey coal stratigraphic database—the database and interactive map: Indiana Geological Survey report of progress. 2012a; 39 CD-ROM.
6. Drobniak A, Mastalerz M. The Indiana coal quality database—the database and interactive map: Indiana Geological Survey report of progress. 2012b; 40 CD-ROM.
7. Drobniak A, Mastalerz M. Interactive map of the Seelyville Coal Member in Indiana: Indiana Geological Survey report of progress. 2014; 47:17.
8. Elder CH, Deul M. Degasification of Mary Lee Coalbed, near Oak Grove, Jefferson County, Alabama, by vertical borehole in advance of mining. U.S. Bureau of Mines, report of investigations. 1974; 7968

Author Manuscript Author Manuscript Author Manuscript Author Manuscript

9. Fekete Associates, Inc. F.A.S.T. CBM. Calgary (Alberta, Canada): 2012.
10. Ham, YS., Kantzas, A. CIPC/SPE gas technology symposium 2008 joint conference. Calgary (Alberta, Canada): Society of Petroleum Engineers; 2008. Development of coalbed methane in Australia: unique approaches and tools. SPE-114992
11. Hower TL. Coalbed-methane reservoir simulation: an evolving science. J Petrol Technol. 2004; 56(4):61–3.
12. Karacan CÖ, Drobniak A, Mastalerz M. Coal bed reservoir simulation with geostatistical property realizations for simultaneous multi-well production history matching: a case study from Illinois Basin, Indiana, USA. Int J Coal Geol. 2014; 131:71–89.
13. Karacan CÖ, Olea RA, Goodman GVR. Geostatistical modeling of gas emissions zone and its in-place gas content for Pittsburgh seam mines using sequential Gaussian simulation. Int J Coal Geol. 2012; 90–91:50–71.
14. Karacan CÖ, Olea RA. Time-lapse analysis of methane quantity in the Mary Lee group of coal seams using filter-based multiple-point geostatistical simulation. Math Geosci. 2013; 45:681–704. [PubMed: 26191095]
15. Karacan CÖ, Ruiz FA, Cotè M, Phipps S. Coal mine methane: a review of capture and utilization practices with benefits to mining safety and to greenhouse gas reduction. Int J Coal Geol. 2011; 86:121–56.
16. Karacan CÖ. Integration of vertical and in-seam horizontal well production analysis and stochastic geostatistical algorithms to estimate pre-mining methane drainage efficiency from coal seams Blue Creek seam Alabama. Int J Coal Geol. 2013; 114:96–113. [PubMed: 26435557]
17. Karacan CÖ. Production history matching to determine reservoir properties of important coal groups in the Upper Pottsville formation, Brookwood and Oak Grove fields, Black Warrior Basin, Alabama. J Nat Gas Sci Eng. 2013; 10:51–67. [PubMed: 26191096]
18. Karacan CÖ. Development and application of reservoir models and artificial neural networks for optimizing ventilation air requirements in development mining of coal seams. Int J Coal Geol. 2007; 72:221–9.
19. Karacan CÖ. Evaluation of the relative importance of coal bed reservoir parameters for prediction of methane inflow rates during mining of longwall development entries. Comput Geosci. 2008; 34(9):1093–114.
20. Karacan CÖ. Modeling and analysis of gas capture from sealed sections of abandoned coal mines. Int J Coal Geol. 2015; 138:30–41.
21. King GR, Ertekin T, Schwerer FC. Numerical simulation of the transient behavior of coal-seam degasification wells. SPE Form Eval. 1986:165–83.
22. Mastalerz M, Drobniak A, Rupp JA, Shaffer NR. Characterization of Indiana's coal resource: availability of the reserves, physical and chemical properties of the coal and present and potential uses. Indiana Geological Survey, special report. 2009; 66:45.
23. Moore TA. Coalbed methane: a review. Int J Coal Geol. 2012; 101:36–81.
24. Pyrcz, MJ., Deutsch, CV. Geostatistical reservoir modeling. 2. Oxford University Press; 2014. p. 433
25. Remy, N., Boucher, A., Wu, J. Applied geostatistics with SGeMS: a user's guide. Cambridge (United Kingdom): Cambridge University Press; 2009. p. 264
26. Salmachi A, Sayyafzadeh M, Haghighi M. Infill well placement optimization in coal bed methane reservoirs using genetic algorithm. Fuel. 2013; 111:248–58.
27. Smith DH, Bromhal G, Sams WN, Jikich S, Ertekin T. Simulating carbon dioxide sequestration/ECBM production in coal seams: effects of permeability anisotropies and the diffusion-time constant. SPE Reservoir Eval Eng. 2005; 8(2):156–63.
28. Strąpoć D, Mastalerz M, Schimmelmann A, Drobniak A, Hedges S. Variability of geochemical properties in a microbially dominated coalbed gas system from the eastern margin of the Illinois Basin USA. Int J Coal Geol. 2008; 76:98–110.

Author Manuscript Author Manuscript Author Manuscript Author Manuscript

HIGHLIGHTS

- Coal property realization was used.
- CBM reservoir simulations were conducted.
- History match errors were quantified.
- Uncertainty in results was evaluated.
- Most likely representations of coal properties were determined.

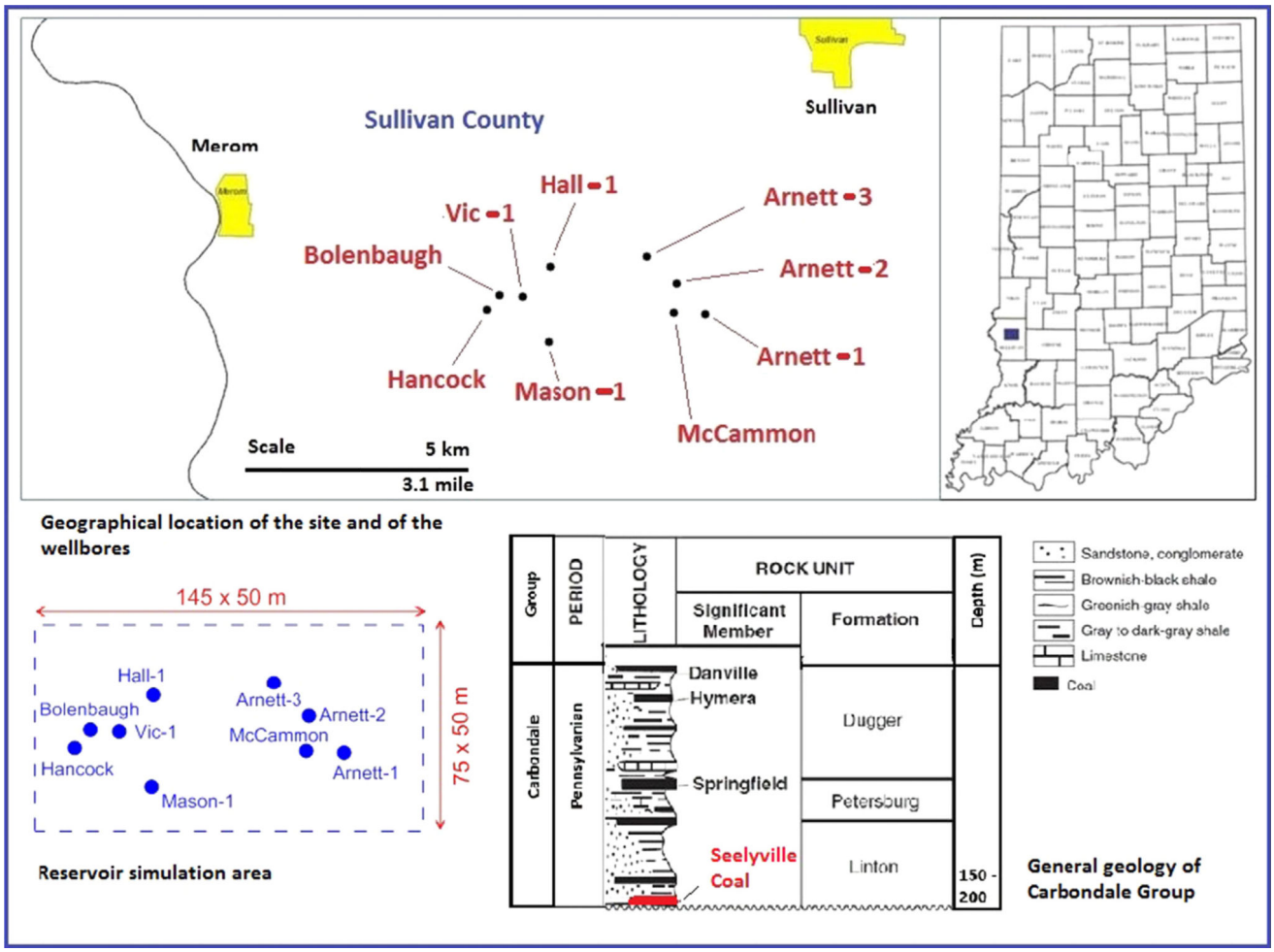

Fig. 1.

Location of study area with the coalbed methane wells. General geology of the Carbondale group where Seelyville coal is located and the boundaries and size of the modeled area are also shown.

Author Manuscript Author Manuscript Author Manuscript Author Manuscript

Author Manuscript Author Manuscript Author Manuscript Author Manuscript

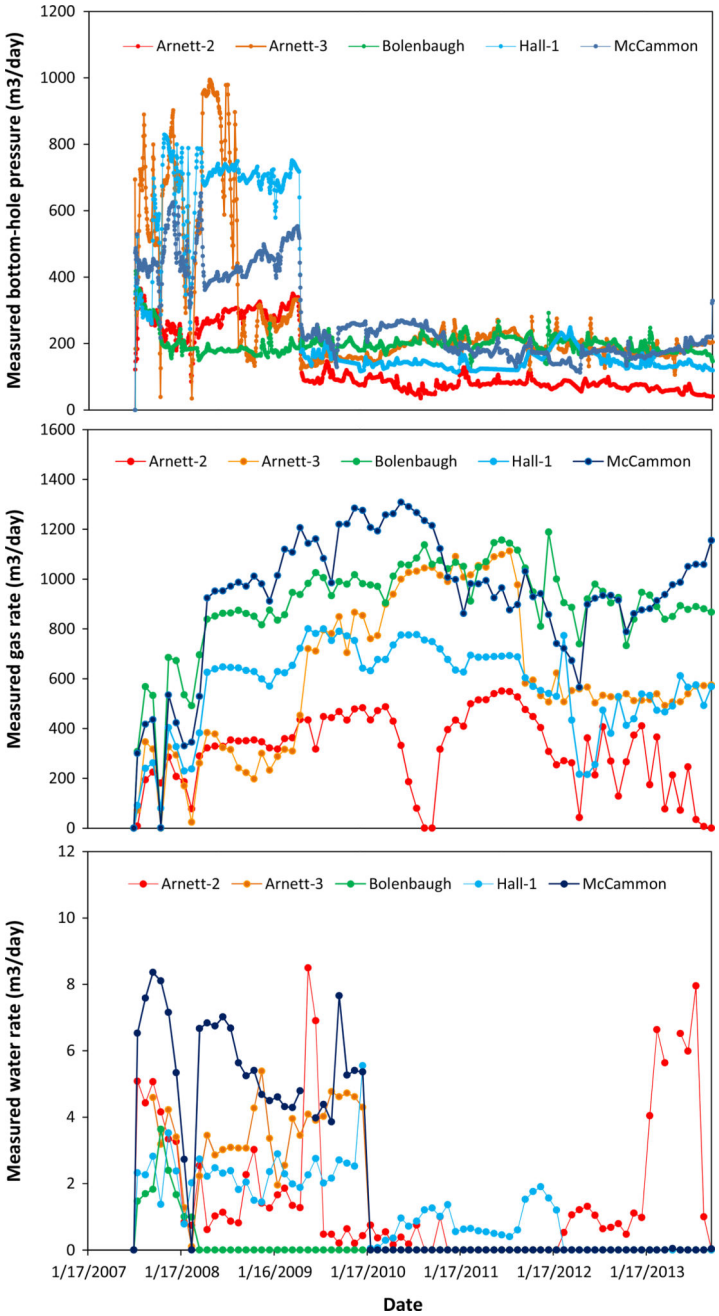

Fig. 2.

Measured bottom-hole pressure, gas, and water rate data of 5 of the studied wells between July 2007 and October 2013.

Author Manuscript Author Manuscript Author Manuscript Author Manuscript

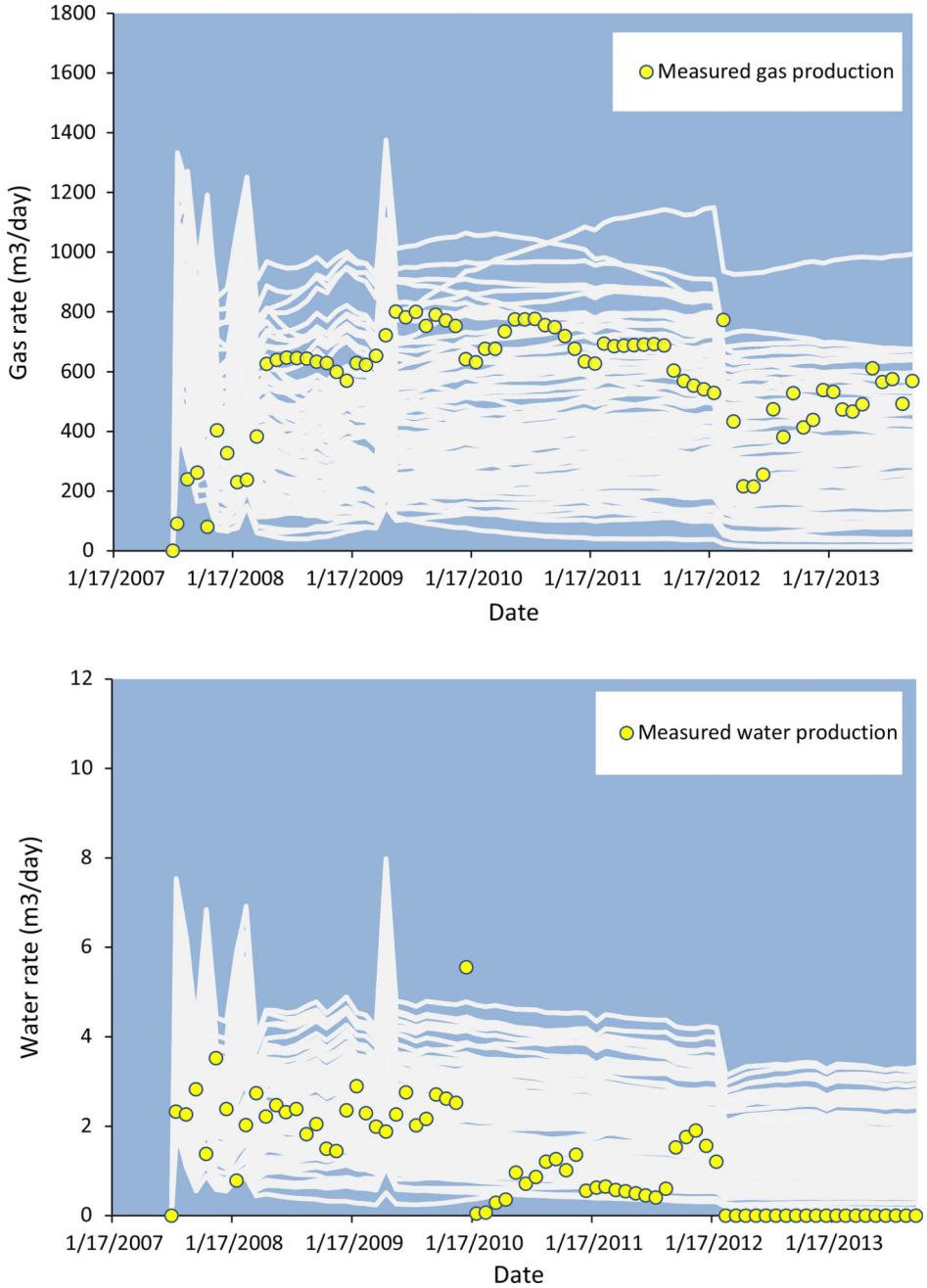

Fig. 3.

Simulated gas and water production rates for all 100 simulations (light-colored lines) in comparison with the measured data for Hall-1. (For interpretation of the references to color in this figure legend, the reader is referred to the web version of this article.)

Author Manuscript Author Manuscript Author Manuscript Author Manuscript

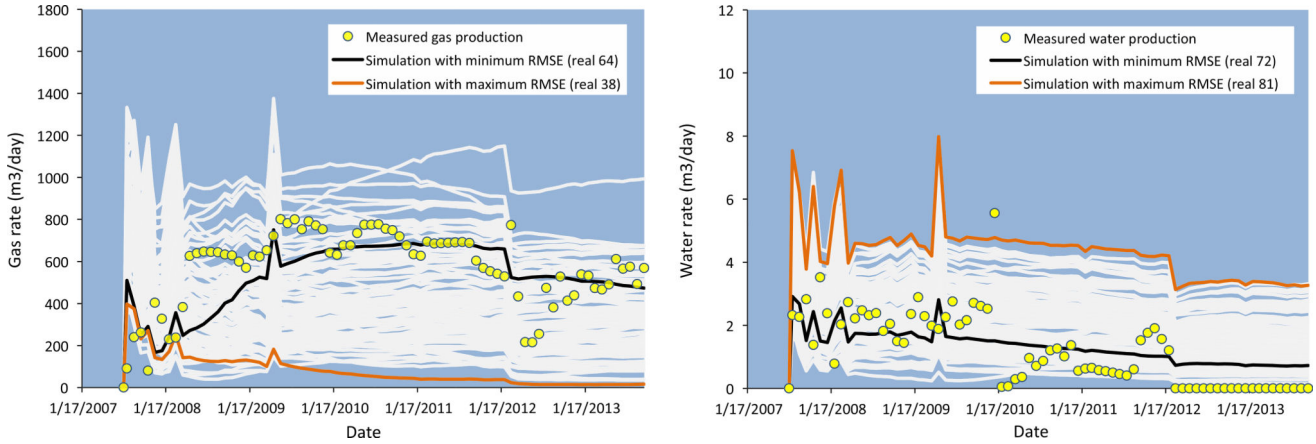

Fig. 4.

Results of the match between simulated rates and the measured ones using realization bundles 64 and 38 for gas rate and 72 and 81 for water rate, which gave minimum and maximum errors for Hall-1.

Author Manuscript Author Manuscript Author Manuscript Author Manuscript

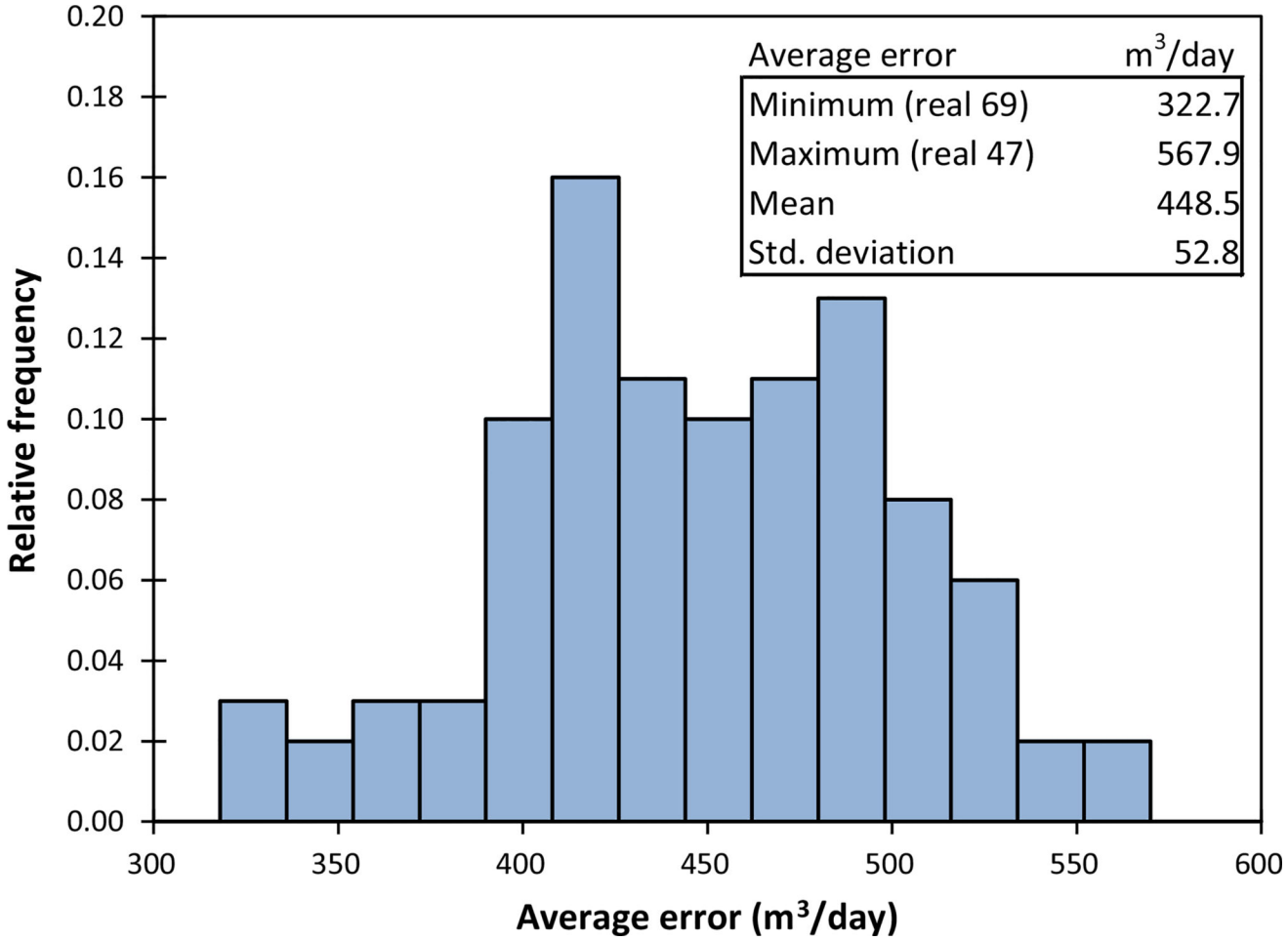

Fig. 5.
Distribution of average history matching errors (based on gas rate) calculated using Eq. (2).

Author Manuscript Author Manuscript Author Manuscript Author Manuscript

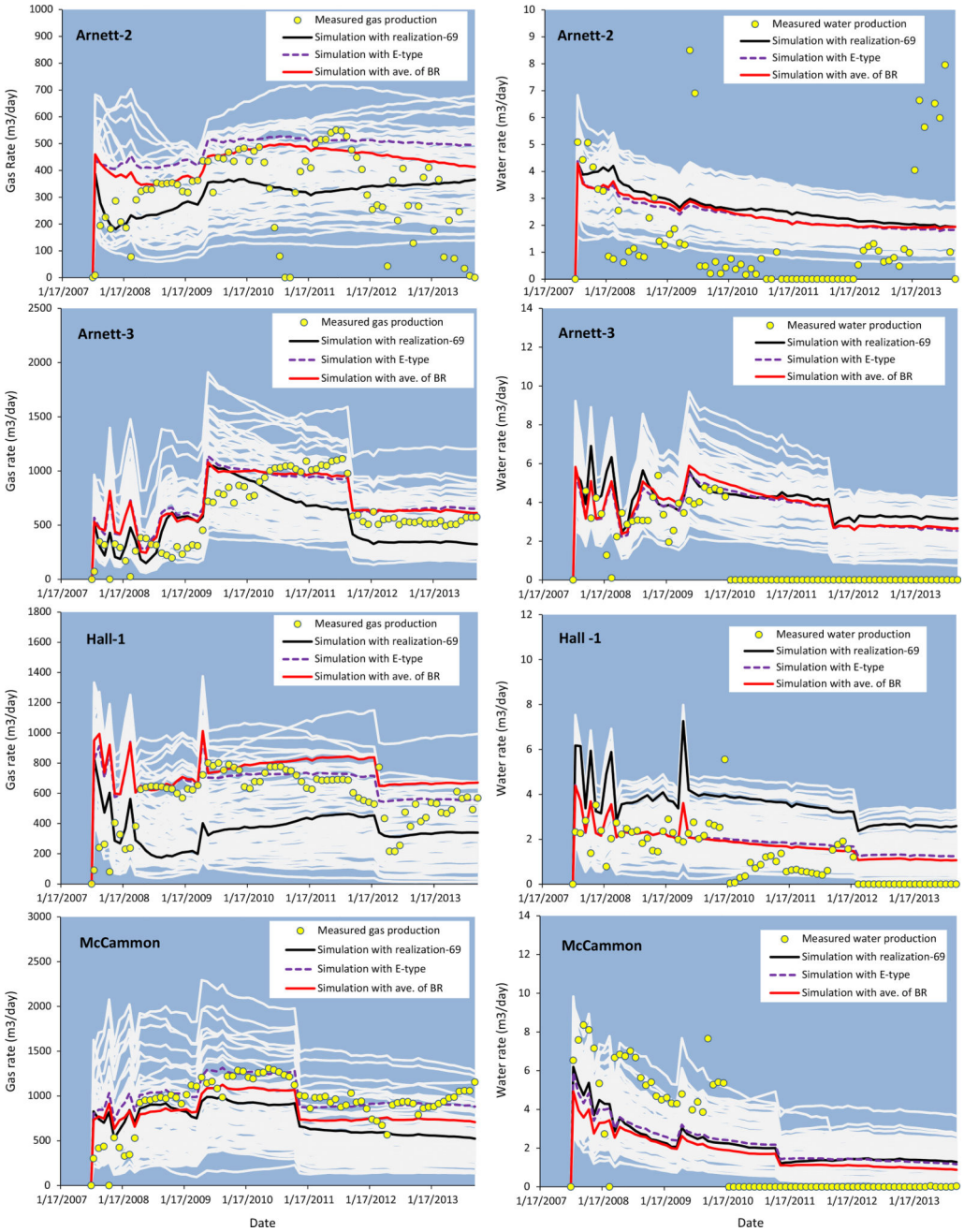

Fig. 6.

Comparison of predicted gas and water rates using realization 69, E-type, and average of best realizations (BR in the legends) with the measured values for four of the wells.

Author Manuscript Author Manuscript Author Manuscript Author Manuscript

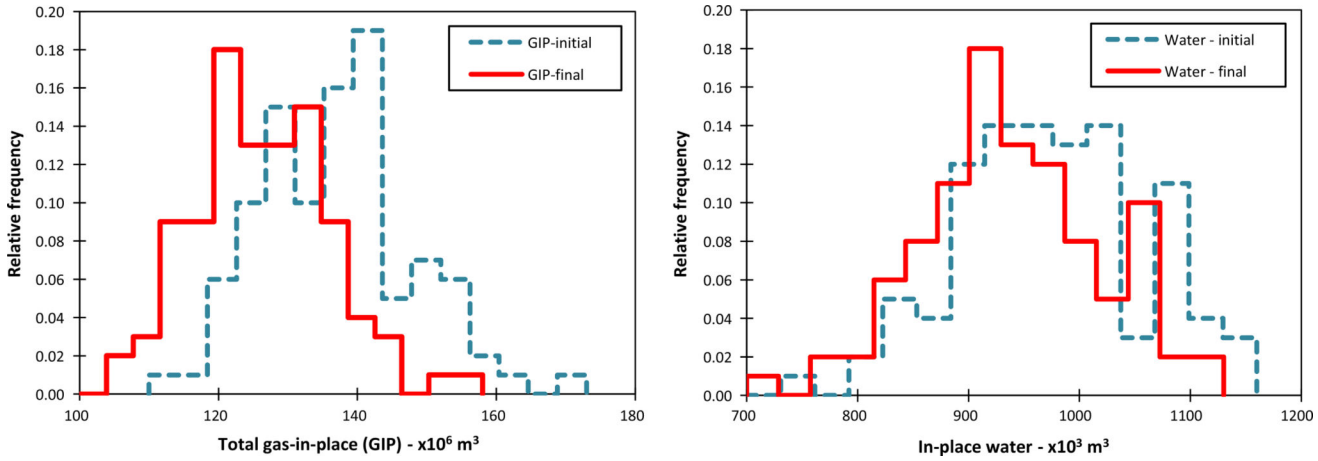

Fig. 7.
Histograms of initial gas-in-place and water within the model area.

Author Manuscript Author Manuscript Author Manuscript Author Manuscript

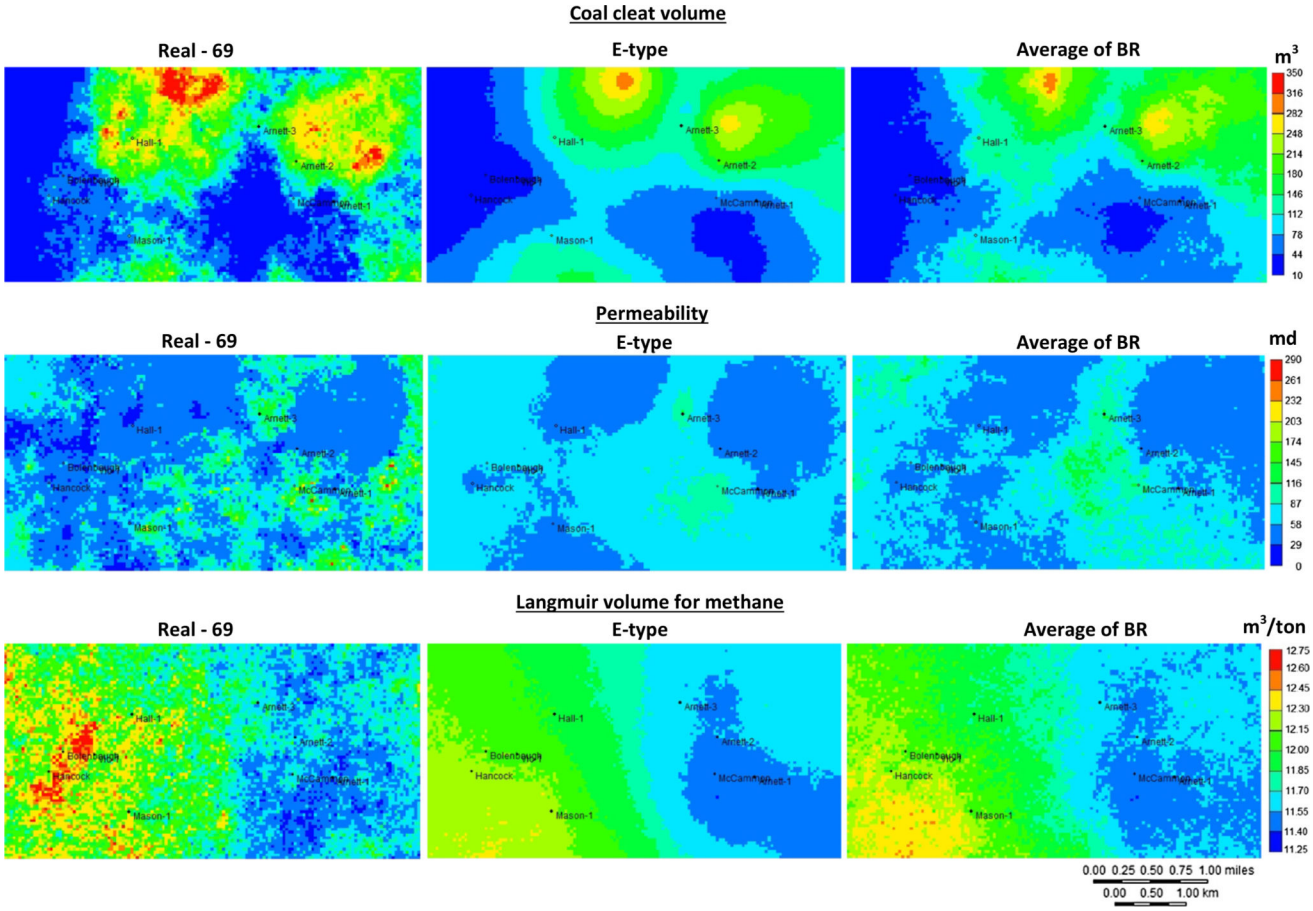

Fig. 8.

Maps of three different coal attributes for real 69, E-type, and average of best realizations (BR).

Author Manuscript Author Manuscript Author Manuscript Author Manuscript

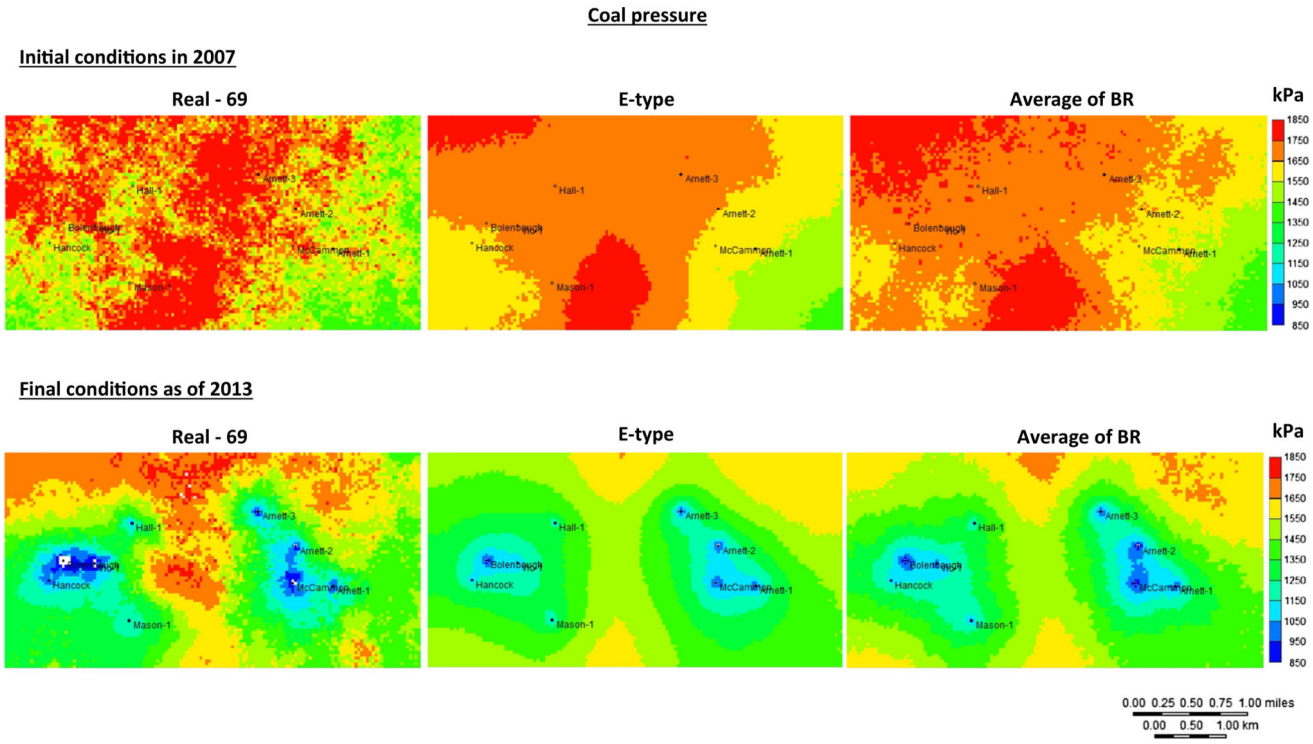

Fig. 9.

Maps of pressure distributions in 2007 and 2013 in real 69, E-type, and average of best realizations.

Author Manuscript Author Manuscript Author Manuscript Author Manuscript

Table 1

Statistical results of the errors in gas (top) and water rates (lower) after 100 simulations, as well as the realization bundles that give minimum and maximum error for each wellbore.

Wellbore	Number of realizations	Min. error (m^3/day)	Max. error (m^3/day)	Mean error (m^3/day)	Std. dev. of error (m^3/day)
Arnett-1	100	169.6 (real 3)	1186.9 (real 98)	356.0	177.2
Arnett-2	100	131.8 (real 45)	336.3 (real 46)	184.6	34.9
Arnett-3	100	132.3 (real 12)	638.9 (real 62)	298.6	85.6
Bolenbaugh	100	181.6 (real 60)	840.4 (real 34)	437.5	129.2
Hall-1	100	154.9 (real 64)	537.9 (real 38)	323.8	87.0
Hancock	100	87.0 (real 90)	736.3 (real 91)	217.2	127.6
Mason-1	100	218.0 (real 41)	1422.0 (real 77)	982.3	310.9
McCammon	100	173.9 (real 43)	844.1 (real 21)	466.6	142.8
Vic-1	100	433.4 (real 76)	1022.5 (real 89)	769.7	149.4
Arnett-1	100	24.8 (real 28)	25.3 (real 17)	25.1	0.1
Arnett-2	100	2.3 (real 24)	3.1 (real 27)	2.6	0.2
Arnett-3	100	16.9 (real 7)	17.4 (real 47)	17.2	0.1
Bolenbaugh	100	0.5 (real 44)	2.2 (real 76)	0.9	0.4
Hall-1	100	0.9 (real 72)	3.3 (real 81)	1.6	0.6
Hancock	100	0.6 (real 68)	2.9 (real 87)	0.8	0.3
Mason-1	100	0.1 (real 63)	1.5 (real 0)	0.4	0.3
McCammon	100	2.4 (real 25)	3.7 (real 46)	2.8	0.2
Vic-1	100	0.7 (real 34)	2.2 (real 98)	1.0	0.3

Author Manuscript Author Manuscript Author Manuscript Author Manuscript

Table 2

Gas and water production rate errors from simulations conducted by using realization 69, E-type, and average of the best realizations.

Wellbore	Error $(\overline{\overline{\mathrm{RMSE}}})$ for gas data (m^3/day)			Error $(\overline{\overline{\mathrm{RMSE}}})$ for water data (m^3/day)		
	Real-69	E-type	Ave. of best realizations	Real-69	E-type	Ave. of best realizations
Arnett-1	202.2	183.1	171.0	25.0	25.0	25.0
Arnett-2	149.8	221.9	186.2	2.6	2.5	2.5
Arnett-3	255.5	231.9	215.0	17.2	17.2	17.1
Bolenbaugh	283.9	264.8	284.1	0.9	0.7	0.9
Hall-1	311.5	217.8	260.5	2.6	1.2	1.1
Hancock	361.1	195.5	145.5	0.8	0.7	0.8
Mason-1	481.9	771.3	459.3	0.1	0.1	0.1
McCammon	325.9	220.3	239.4	2.7	2.6	2.7
Vic-1	534.3	482.8	567.5	1.5	0.8	0.8
$\overline{\overline{\mathrm{RMSE}}}$	322.7	309.9	281.0	5.9	5.7	5.7

Author Manuscript Author Manuscript Author Manuscript Author Manuscript

Table 3

Quantile values and basic statistics of GIP and water quantities, based on 100 realization bundles, presented in Fig. 7.

Quantile	GIP-initial ($\times 10^6$ m^3)	GIP-final ($\times 10^6$ m^3)	In-place water-initial ($\times 10^3$ m^3)	In-place water-final ($\times 10^3$ m^3)
Q95	154.3	142.5	1108.5	1067.0
Q90	151.5	137.9	1089.8	1051.4
Q75	142.9	132.0	1024.0	990.2
Q50	137.1	125.8	970.3	934.1
Q25	129.2	119.5	915.1	886.0
Q10	123.0	114.6	862.7	832.3
Q5	121.7	111.3	835.6	812.5
Minimum	112.4	105.3	735.1	705.3
Maximum	172.4	157.9	1158.8	1125.0
Mean	137.0	126.4	974.0	940.1
Std. dev.	10.6	9.6	83.9	81.4

Author Manuscript

Author Manuscript

Author Manuscript

Author Manuscript

Table 4

Initial and final GIP and water quantity calculated for the study using realization bundle 69, E-type, and average of best realizations.

	Real-69	E-type	Ave. of best realizations
GIP ($\times 10^6$ m^3)-initial	151.5	137.5	139.8
GIP ($\times 10^6$ m^3)-final	138.9	123.3	125.7
In-place water ($\times 10^3$ m^3)-initial	1036.5	910.0	901.9
In-place water ($\times 10^3$ m^3)-final	997.4	878.6	870.9